



ELSEVIER

Agricultural and Forest Meteorology 94 (1999) 171–188

**AGRICULTURAL
AND
FOREST
METEOROLOGY**

Below-canopy and soil CO₂ fluxes in a ponderosa pine forest

B.E. Law^{a,*}, D.D. Baldocchi^b, P.M. Anthoni^c^aDepartment of Forest Science, Peavy Hall 154, Oregon State University, Corvallis OR 97331, USA^bAtmospheric Turbulence and Diffusion Division, NOAA, PO Box 2456, Oak Ridge TN 37831, USA^cCollege of Oceanic and Atmospheric Sciences, Strand Agriculture Hall 326, Oregon State University, Corvallis OR 97331, USA

Received 10 November 1997; received in revised form 28 January 1999; accepted 28 January 1999

Abstract

Below-canopy eddy covariance measurements of CO₂ flux (F_{cb}) and soil surface CO₂ flux measurements (F_s) were made seasonally in a ponderosa pine forest in central Oregon in 1996 and 1997. The forest ecosystem has a very open canopy, and it is subject to drought and high vapor pressure deficits in summer. Below-canopy flux measurements in March, May, and August 1997 showed increasing effluxes from the forest floor as soils warmed. In July 1996, daytime F_{cb} measurements appeared to have been influenced by photosynthetic uptake of CO₂ by ground vegetation. We did not see a similar diurnal trend in F_{cb} data in August 1997, probably because photosynthesis may have decreased with senescence of $\sim 1/3$ of the pine canopy and the herbaceous species. On 4 days in August 1997, the mean nocturnal F_s ($2.6 \pm 0.08 \mu\text{mol m}^{-2} \text{s}^{-1}$) was lower than nocturnal F_{cb} ($3.5 \pm 0.28 \mu\text{mol m}^{-2} \text{s}^{-1}$) by 26%, and daytime F_s was lower than nocturnal F_{cb} by 18%, possibly because F_{cb} includes respiration by understory and the lower portions of trees. The mean nocturnal NEE calculated from above-canopy flux and storage in the canopy airspace ($F_{ca} + F_{stor}$) at this time was $2.8 \pm 0.40 \mu\text{mol m}^{-2} \text{s}^{-1}$, 23% lower than ecosystem respiration calculated from chamber measurements on soils, wood, and foliage. The largest difference was observed on a more a turbulent night ($u_* = 0.30 \text{ m s}^{-1}$) when $F_{ca} + F_{stor}$ was even significantly less than F_{cb} and F_s . Our hypothesis is that under calm conditions (e.g. $u_* < 0.15 \text{ m s}^{-1}$ as observed on three of the nights), F_{ca} is negligible and has no impact on the CO₂ budget. Under weak wind conditions (e.g. $u_* = 0.30 \text{ m s}^{-1}$), F_{ca} begins to become significant and fluxes missed by the above-canopy eddy correlation system degrade the CO₂ budget. Under windy conditions, the above-canopy eddy correlation measurement is a good approximation and the CO₂ budget improves again. Below-canopy flux measurements provided useful temporal information for understanding seasonal differences in diel patterns, while the chambers allowed us to characterize spatial variation in CO₂ fluxes. It is important to measure below-canopy fluxes along with above-canopy fluxes throughout the year to understand CO₂ exchange components and annual contributions to the carbon budget of open canopy forest systems. © 1999 Elsevier Science B.V. All rights reserved.

Keywords: Carbon dioxide; Ecophysiology; Soil CO₂ fluxes; Eddy covariance; Pine forests; *Pinus ponderosa*

1. Introduction

Net ecosystem exchange (NEE) is the difference between gross uptake of CO₂ by plants and that released to the atmosphere from respiration by autotrophs (R_a) and heterotrophs (R_h). The processes con-

*Corresponding author: Tel.: +1-541-737-2996; fax: +1-541-737-2540; e-mail: lawb@ccmail.orst.edu

trolling NEE operate on a variety of time and spatial scales and are influenced by many environmental variables such as temperature, moisture, nutrients, frequency and type of disturbance. Soil CO₂ efflux (F_s) results from the metabolic activities of roots, mycorrhizae, decomposers, and other soil organisms, and can contribute substantially to NEE. Rhizosphere respiration has been estimated to be 25–45% of gross primary productivity (GPP) in a range of pine ecosystems, and 48–71% of ecosystem respiration (Raich and Schlesinger, 1992; Lavigne et al., 1997; Schlesinger, 1997). In the ponderosa pine forest, scaled-up chamber measurements showed that soil CO₂ effluxes were responsible for 76% of annual ecosystem respiration, and on windy nights, above-canopy eddy covariance estimates of NEE (F_{ca} + change in CO₂ storage) were lower than chamber estimates by 50% (Law et al., 1999). Thus it is critical to improve our understanding of processes controlling soil CO₂ effluxes, and to improve estimates of nocturnal fluxes, which have a large impact on annual NEE.

Most soil CO₂ production occurs in the surface litter and surface layer of soil (<15 cm depth), where decomposition is rapid and a large portion of the fine root biomass exists (Edwards and Sollins, 1973; Singh and Gupta, 1977; Bowden et al., 1993). Processes that influence below-canopy CO₂ flux measurements (F_{cb} ; 2 m measurement height) include decomposition, photosynthesis and respiration by the understory (if present) and the lower portion of overstory trees. Respiration by stems and branches, however, contributes only ~5% of total ecosystem respiration per m² ground, and averages <1 μmol m⁻² s⁻¹ in summer at our study site, so its influence on F_{cb} is negligible (Law et al., 1999).

Several studies have used environmental variables to estimate soil CO₂ fluxes (Šimuněk and Suarez, 1993; Nakane, 1994). These studies have shown that F_s is primarily a function of soil temperature, and many have used the exponential dependence of F_s on soil temperature to develop models (Raich and Schlesinger, 1992). Soil moisture also influences autotrophic and heterotrophic soil processes. Burton et al. (1998) showed that soil moisture deficits decreased root respiration up to 17%, and Goulden et al. (1996) showed that heterotrophic respiration decreased more than autotrophic respiration during extended drought in a temperate deciduous forest. Decomposition rates

have been correlated with the carbon : nitrogen ratio and lignin : nitrogen ratio of soils, with reduced decomposition rates at higher ratios (Melillo et al., 1982).

Below-canopy CO₂ flux measurements using micrometeorological methods (Baldocchi and Vogel, 1996; Black et al., 1996) are quasi-continuous and useful for explaining diel and seasonal variation in ecosystem processes near the forest floor. They are also useful for interpreting sources of carbon and water vapor fluxes measured above the forest canopy. Chamber measurements of F_s at the soil surface are labor-intensive, but valuable for evaluating spatial variation and distinguishing soil surface fluxes from other sources (e.g. understory). The combination of chamber measurements with above- and below-canopy flux measurements can be a powerful approach to understanding temporal and spatial variation in ecosystem flux components.

Ecosystem carbon and water vapor flux measurements and related biological and microclimate measurements have been made for more than 2 years in a ponderosa pine forest in central Oregon. The project's overall objectives are to improve understanding of the contributions of ecosystem components to fluxes, to investigate responses of ecosystem processes to climatic variables, and to evaluate ecosystem models. This forest ecosystem is particularly constrained by soil moisture deficits and high vapor pressure deficits in summer. Over 2 years, we have periodically measured F_{cb} by the eddy covariance method and F_s with chambers along with making above-canopy flux measurements. In this paper, we evaluate different statistical models for estimating F_s from measurements of abiotic factors such as soil temperature and moisture, and nitrogen and carbon in the soil and litter layers. We report on the diel, seasonal, and spatial variation in F_{cb} and F_s in the ponderosa pine ecosystem, and compare methods of measuring CO₂ fluxes below the canopy. Finally, results are compared with data from other forests where below-canopy fluxes have been measured.

2. Methods

2.1. Site description

The site is a ponderosa pine (*Pinus ponderosa*) forest in central Oregon, located in the Metolius

Research Natural Area (44°30'N, 121°37'W, elevation 940 m). The terrain is nearly flat with a slope between 2 and 6%, except for a north–south ridge about 1 km to the east of the site. The pine forest extends at least 12 km in all directions.

Ponderosa pine exists over a broad range of temperature regimes, from a Mediterranean climate (e.g. California) to the colder Rocky Mountain region (e.g. Montana, Wyoming) (Knight et al., 1994). Ponderosa pine forests are xeromorphic, occurring where annual precipitation is ~600 mm or less. Xeromorphic pines typically occur on coarse-textured soils, which allow water to infiltrate rapidly rather than evaporating from the surface (Knight et al., 1994). The soil at our site is classified as a light-colored andic (high in ash content) inceptisol that is low in nutrients. Our texture analysis showed the soil is 73% sand, 21% silt, and 6% clay. Fine roots occur primarily in the top 20 cm of the soil (Ted Dyrness, pers. comm.).

The ponderosa pine forest consists of stands of two distinct age classes, with 27% of the area in old trees (~250 years), 25% younger trees (~45 years) and 48% a mix of these age classes (Table 1). The canopies of the old and mixed stands are very open. The understory is sparse with patches of bitterbrush (*Purshia tridentata*), bracken fern (*Pteridium aquilinum*) and strawberry (*Fragaria vesca*). The leaf area index (LAI; m² needle half-surface area m⁻² ground) of the trees, calculated from optical measurements corrected for foliage clumping, ranged from 0–5 across the site, with a mean of 1.5 ± 0.1 in summer (Law et al., in prep.). This is low but typical of relatively undisturbed ponderosa pine forests in Oregon.

Total precipitation was 595 mm in 1996 and 198 mm in 1997. Long-term climate records from a nearby weather station (Sisters, OR) indicate that the 1996 precipitation was about 162% of the normal annual total (1961–1990). Mean annual temperature was about the same in both years (8.4–8.5°C).

2.2. Eddy covariance

2.2.1. Measurements

Half-hourly eddy covariance measurements of below-canopy CO₂, water vapor and sensible heat fluxes were made for several periods through the year in a mixed stand of young and old *P. ponderosa*, at a position 2.0 m above the forest floor. We selected periods that would capture seasonal changes in climate and ecosystem processes, July 1996, March, May, and August 1997. Carbon dioxide and water vapor were measured with an open-path infrared gas analyzer (IRGA; NOAA ATDD, Oak Ridge, TN), which responds to frequencies up to 15 Hz for both scalars and has a low noise-to-signal ratio (less than 300 µg m⁻³ for CO₂; Auble and Meyers, 1992). Standard mixtures of CO₂, traceable to a World Meteorological Organization (WMO) standard, were used for calibration.

In July 1996 (Days 187–205), wind velocity and virtual temperature fluctuations were measured with a three-dimensional sonic anemometer (Solent 1012 R2, Gill Instruments, Lymington, England). The analog signals were digitized at 21 Hz with hardware on the sonic anemometer and calculated at 10 Hz on a laptop computer. Micrometeorological flux data were

Table 1
Tree and stand characteristics (means with standard errors in parentheses)

	Young stands	Old stands
Age of trees	45	250
Trees per hectare	550	70
Tree height (m)	9 (0.2)	33 (0.8)
Diameter breast height (cm)	12.1 (0.2)	63.3 (2.7)
Leaf area index (m ² m ⁻²)	1.5 (0.1)	1.5 (0.1)
Sapwood volume (m ³ ha ⁻¹)	22 (0.3)	223 (10)
Soil Nitrogen (%)	0.15 (0.03)	0.10 (0.03)
Humus Nitrogen (%)	0.97 (0.28)	0.59 (0.16)
Litter C : N	51 (6)	46 (6)
Annual litterfall biomass (g m ⁻²)	315 (49)	194 (28)
Mean annual soil temperature (°C at 15 cm)	9.4	11.0
Mean annual soil water content (m ³ m ⁻³ at 0–30 cm depth)	0.15	0.14

digitized, processed and stored using in-house software (Baldocchi et al., 1988). In March, May, and August 1997 (Days 78–89, 129–151 and 220–234), we operated the flux system with a Campbell Scientific three-dimensional sonic anemometer (Model CSAT-3, Campbell Scientific, Logan, UT). Covariances and statistics were calculated by a CR10X datalogger (Campbell Scientific, Logan, UT) running at 8 Hz in spring and 10 Hz in summer.

Eddy covariance measurements of CO₂ fluxes were also made at 47 m height (13 m above the canopy), and half-hourly mean CO₂ concentration profile measurements were made at four heights (1, 8, 31, and 46 m). Wind velocity was measured with a Solent sonic anemometer. The change in CO₂ storage (F_{stor}) in the canopy airspace was combined with flux measurements to estimate NEE. The instrumentation, flux corrections and calculations were reported in Law et al. (1999) and Anthoni et al. (1999). Flux footprint analysis under neutral conditions suggests that a majority of the fluxes come from within 800 m of the tower, and the footprint extends to approximately 1 km (Baldocchi, 1997; Law et al., 1999). Our soil chamber and below-canopy flux measurements were made 300 m from the tower, within the potential footprint.

Soil temperature was measured with two multi-level thermocouple probes; sensors were 0.02, 0.04, 0.08, 0.16 and 0.32 m below the surface. Photosynthetically active radiation (PAR) and net radiation were measured with a quantum sensor (Model LI-190S, LICOR, Lincoln, NE) and a net radiometer (Model Q7, REBS, Seattle, WA), respectively. To reduce errors from the spatially variable radiation of the open canopy, the instruments were mounted on a tram that traveled 30 m back and forth 1 m above the forest floor. The length and speed of the traverse were chosen to minimize the coefficient of variation of the spatial samples. A reading was taken every second, corresponding to a distance of 2 cm between readings. Air temperature and relative humidity were measured with a Model HMP-35C instrument (Vaisala, Helsinki, Finland) placed alongside the flux instrumentation.

2.2.2. Computations

Vertical flux densities of CO₂ (F_c), latent heat (LE) and sensible heat (H) between the forest and the

atmosphere are proportional to the mean covariance between vertical velocity (w') and the scalar (c') fluctuations (CO₂, water vapor, and temperature). In the convention of eddy flux measurements, positive net exchange values represent transfer away from the surface (efflux), and negative values represent transfer towards the surface. Turbulent fluctuations were computed as the difference between instantaneous and mean scalar quantities. During the 1996 summer study, the mean scalar values were determined in real-time, using a digital recursive filter with a 400 s time constant. The mass and energy flux covariances were computed at 30 min intervals. The half-hour covariances of the CSAT-3 system were computed by averaging three 10 min subinterval covariances. Numerical coordinate rotations of the three orthogonal wind axes of the anemometer were applied to align the vertical velocity measurement normal to the mean wind streamlines (Baldocchi et al., 1988). The CO₂ and water vapor flux covariances were corrected for density fluctuations arising from variations in temperature and humidity (Webb et al., 1980) and for influences of horizontal wind speed on virtual temperature (Schoanus et al., 1983). The data were then screened to remove measurements taken when the power supply voltage was below 11.25 V, IRGA water vapor and CO₂ signals were outside the range of the data logger analog inputs, or sampling over the half-hour was incomplete. The flux data were averaged hourly over each of the seasonal measurement periods (12 to 19 days) to reduce noise in the measurements and to ensure enough continuous data remained following the screening.

2.2.3. Eddy covariance system comparisons

Since different sonic anemometers were used for below-canopy measurements in 1996 and 1997 and different methods were used for calculating covariances, we compared the instruments and the calculation methods. Recalculating the 1996 raw eddy covariances of w' and the scalar fluctuations with the 1997 methods showed no significant difference between the two methods. Regressions between the covariances of vertical wind speed with CO₂, water vapor and virtual temperature calculated from both methods had a slope of >0.99 and an intercept of ~0.0 ($r^2 > 0.99$, $n = 107$) indicating good agreement between the methods.

In September 1997, we also compared the two sonic anemometers of the same design side-by-side at the below-canopy flux site for 2 days, with the systems about 1 m apart. There was good agreement between the two systems. Regression between the half-hourly covariances of the vertical wind component with temperature calculated from the two systems showed that the covariance from the Solent system was 2% higher than that from the CSAT-3 system ($r^2 = 0.94$, slope = 0.98, zero intercept, $n = 85$). Regression of the CO_2 fluxes showed that the fluxes that were measured with the Solent system were 10% higher than those measured with the CSAT-3 system ($r^2 = 0.90$, slope = 0.90, zero intercept, $n = 85$). As the 10% difference is within the error uncertainty for flux measurements (Moncrieff et al., 1996), we did not adjust any of the 1996 or 1997 CO_2 fluxes.

2.2.4. Source area of below-canopy flux system

The footprint of below-canopy flux measurements was estimated to determine site characteristics upwind of the instruments. We used a Lagrangian random walk model that simulates the two-dimensional transport of marked fluid parcels that have been released from the soil (Balocchi, 1997). The horizontal distances that the parcels travel between release and reaching the 2 m measurement height was computed as a function of the mean horizontal wind velocity, the standard deviation of vertical velocity fluctuations and the Lagrangian turbulence time scale. We evaluated the footprint for daytime atmospheric conditions (neutral).

2.3. Chamber measurements

We measured CO_2 fluxes from soils, foliage and wood with chambers periodically through the year to estimate hourly respiration rates for each component, and to investigate possible influences on F_{cb} .

2.3.1. Soil surface CO_2 efflux

Soil surface CO_2 effluxes were measured on 28 days from May 1996 to August 1997 with a LICOR 6200 IRGA operating as a closed system and a LICOR 6000-09 chamber (1152 cm³ volume, 72 cm² surface area; LICOR, Lincoln, NE). Pressure differences may influence F_{s} measurements, but this appears to be

more of an issue for open gas-exchange configurations (Fang and Moncrieff, 1998).

During the growing season, we measured F_{s} at three sample points in each of the five stands of young, old and mixed-age trees (45 sample points). We continued measurements at two stands of each type through the winter when snow was absent from the plots. The plots were distributed over a 600 m × 1200 m area, centered on the above-canopy eddy covariance tower. For comparisons with F_{cb} measurements, we also measured F_{s} at three collars within 30 m of the eddy covariance system approximately every 2 h over 4 days and nights in August 1997. We removed live vegetation inside the chamber collars at least 24 h before measurements to minimize influences of soil disturbance and root injury on the measurements. Before each measurement, the CO_2 level in the sensor cell was drawn down to just below ambient CO_2 concentration (Norman et al., 1992). Five observations were recorded per measurement, and each measurement took ~3 min.

To evaluate statistical models for estimating F_{s} , we used measurements of soil temperature, soil water content, and soil and litter chemistry. We used soil temperature at 15 cm depth obtained from a probe attached to the IRGA chamber and temperature profile measurements. Soil water content was measured using time domain reflectometry (TDR; Tektronix cable tester) at each plot (0–30 cm, and 0–100 cm depths) during the soil chamber measurements. Soil water content was calculated from the TDR measurements using methods described by Timlin and Pachepsky (1996). We measured nitrogen and carbon concentration in the litter, humus and soil layers (0–15 cm soil depth). Litterfall was collected monthly through the year in each stand for annual biomass estimates (Raich and Nadelhoffer, 1989) at each chamber plot. We evaluated existing statistical equations (citations in Table 3) and fitted empirical equations to the data.

2.3.2. Foliage measurements

We measured photosynthetic light response and respiration (F_{f}) by 1-year-old foliage of young ponderosa pine trees (~9 m height), and by strawberry within 20 m of the below-canopy flux tower periodically over the growing season with a LICOR 6400 steady-state infrared gas analyzer (open system; LICOR, Lincoln, NE). Predictive equations for esti-

mating hourly foliage respiration have been evaluated by Law et al. (1999).

Photosynthetic light response curves were developed from measurements at incrementally reduced light levels in the chamber, while temperature and humidity were maintained at constant ambient values. The measurements were automated, and readings were recorded when the coefficient of variation was less than 10%. This procedure allowed the foliage to acclimate to the new light level. Pine needle area (length and width) was measured with callipers and converted to surface area by the constant 2.36, which was calculated from cylinder geometry of the three-needle fascicles. Net assimilation (A_n , $\mu\text{mol m}^{-2} \text{s}^{-1}$) was based on half the total surface area of the needles (HSA). The light response curves were used to estimate hourly assimilation for the below-canopy PAR environment measured by the PAR sensor on the tram. The equation of Landsberg (1986) was applied to fit the light response curves for *P. ponderosa* and *F. vesca*:

$$A_n = \left(\frac{(\alpha_p \cdot \text{PAR} \cdot A_{\text{max}})}{(\alpha_p \cdot \text{PAR}) + A_{\text{max}}} \right) - F_f, \quad (1)$$

where α_p is quantum efficiency of photosynthesis and A_{max} is the maximum photosynthetic rate. We constrained net assimilation by hourly air vapor pressure deficit (VPD) measured at the below-canopy flux system. We assumed no reduction in photosynthesis for $\text{VPD} < 1.5$ kPa, a linear reduction in the scalar between 0 and 1 for $\text{VPD} 1.5\text{--}2.5$ kPa, and no photosynthesis for $\text{VPD} > 2.5$ kPa (Law and Waring, 1994; Waring et al., 1995).

For comparisons with F_{cb} , we scaled chamber measurements of foliage respiration and assimilation by overstory and understory vegetation to unit ground area with leaf area index of each component that was below the 2 m measurement height of the flux system. Percentage cover of the understory was determined by the line intercept method (Law and Waring, 1994), where interception of vegetation by 10 lines attached to a 1 m \times 1 m plot frame was recorded. Thirteen plots were located along two transects running 90 m north and south of the below-canopy flux system. As the understory leaf angle distribution was primarily horizontal with no mutual shading, we calculated LAI ($\text{m}^2 \text{HSA m}^{-2}$ ground) from percentage cover (Law, 1995).

Additional measurements included monthly pre-dawn leaf water potential (Ψ_{predawn}), an indicator of soil water availability to plants (Koide et al., 1991). We shot foliage samples from young and old trees and made measurements with a pressure chamber before sunrise to determine the water potential of non-transpiring foliage.

2.3.3. Wood respiration

We measured woody tissue respiration on the main stems of 10 young trees and 10 old trees periodically through the year. Measurements at 1.5 m height on the stems were made with acrylic chambers and an open path infrared gas analyzer (ADC LCA3, Analytical Development Company, Hoddesdon, England), as described in Law et al. (1999). To calculate F_w per unit volume of sapwood under the chamber, we estimated sapwood volume of each sample tree from allometric equations and sapwood radius of cores collected at the end of the study. Wood respiration was calculated per m^3 sapwood volume under the chamber, then scaled per m^2 ground area from measurements of sapwood volume and trees per m^2 in each age class.

2.3.4. Scaling chamber measurements to the site

The chamber measurements were used in temperature response equations (Table 2) to estimate contributions of foliage, wood and soils to ecosystem respiration at night. Details of scaling up the chamber measurements to the site are described by Law et al. (1999). Below-canopy CO_2 fluxes (F_{cb}) were estimated as the sum of soil surface CO_2 efflux (F_s) plus net assimilation (A_n) by the understory and the lower canopy of young trees plus respiration by the bottom

Table 2

Temperature response models used to estimate hourly CO_2 flux by the ecosystem components

Component	Equation	r^2	Q_{10}
Soils (F_s)	$1.216 \exp(0.059 T_s)$	0.60	1.8
Foliage (F_f)	$0.104 \exp(0.073 T_a)$	0.76	2.1
Wood (F_w)	$2.986 \exp(0.076 T_w)$	0.46	2.1

T_s is soil temperature (0–15 cm depth), T_a is air temperature at 45 m and T_w is sapwood temperature at 2 cm depth in $^{\circ}\text{C}$. Flux rates for soil (F_s) are expressed per m^2 ground per second, for foliage (F_f) per m^2 leaf half-surface area, and for wood (F_w) per m^2 stem surface under the chamber.

2 m of stem sapwood (F_w):

$$F_{cb} = F_s + A_n + F_w \quad (2)$$

where all terms are expressed in $\mu\text{mol m}^{-2}$ ground s^{-1} with the appropriate algebraic sign. The half-hourly chamber estimates of CO_2 fluxes were averaged hourly for comparisons with below-canopy eddy covariance measurements.

3. Results

3.1. Litter and soil measurements

Surface litter was scant in the old stands, and litterfall averaged 38% lower there than in the young stands. Total nitrogen in the mineral soil and humus was also lower in the old stands, by 34 and 39%, respectively (Table 1). During 1996, soil temperature in the old stands was about 15% higher than in the young stands and 13% higher than in the mixed stands. The mean annual soil water content at 0–30 cm was about 10% higher in young stands than in old stands (Table 1). Summer drought typically occurs during July and August; at that time, the mean soil water content was $0.10 \text{ m}^3 \text{ m}^{-3}$ in the old stands and $0.12 \text{ m}^3 \text{ m}^{-3}$ in the young stands. There was 0.6 mm and 11.4 mm of rain during the summer field campaigns in July 1996 and August 1997, respectively.

3.2. Below-canopy eddy covariance measurements

When comparing chamber and micrometeorological methods, it is useful to calculate flux footprints to understand forest characteristics in the source region of fluxes. The footprint for a 2 m measurement height ranged from 2 to 160 m, with 90% of the fluxes coming from within 40 m of the flux system. Generally, our chamber measurements of photosynthesis and F_s for comparisons with F_{cb} were within 30 m of the flux system. The only exception entailed the comparison during July when chamber measurements were obtained across the site.

The energy balance below the canopy can be expressed as

$$R_n = H + \lambda E + G \quad (3)$$

where R_n is net radiation measured by the tram, H is sensible heat flux, λE is latent heat flux, and G is soil heat flux. The slope of the energy balance, $(H + \lambda E)$ plotted against $(R_n - G)$, gives a check on the sensible and latent heat fluxes as measured by eddy covariance against the independently measured variables R_n and G . The slope averaged 0.88 over the July 1996 measurement period (intercept = 15 W m^{-2} , $r^2 = 0.71$, $n = 474$). The slope averaged 0.70 in March and May 1997 (intercept = 11.5, $r^2 = 0.71$, $n = 1377$), with better closure in the afternoon (slope = 0.77, intercept = 17.4, $r^2 = 0.74$, $n = 752$) than morning hours (slope = 0.54, intercept = 6, $r^2 = 0.74$, $n = 625$). The R_n measurement made at 1 m instead of the 2 m height of the flux instruments probably did not have much effect on the energy balance closure because our estimate of the attenuation of shortwave radiation by stems and foliage between the two heights was only 4%.

Large-scale sunflecks measured below the ponderosa pine canopy correspond to the dimension of the forest floor flux footprint. As the sun and shade patches are relatively large and PPFD within them can differ by $1000 \mu\text{mol m}^{-2} \text{ s}^{-1}$, this effect causes the coefficient of determination (r^2) of the surface energy balance closure under the open ponderosa pine stand to be relatively low. In contrast, the dimension of the flux footprint under the jack pine stand is such that mass and energy exchange are averaged over several sun and shade patches, improving the coefficient of determination (Baldocchi and Vogel, 1996).

Fig. 1(a) shows the comparison of diel patterns of below-canopy CO_2 fluxes averaged hourly over July 1996, March, May, and August 1997. During the 24 h period, CO_2 was lost from the forest floor (i.e. F_{cb} was positive) as a result of root and microbial respiration. There were large seasonal differences in the traces. In March, May and August 1997, F_{cb} followed similar diel trends, and mid-day rates were higher as the summer progressed. This agrees with the large seasonal differences in soil temperature (Fig. 1(b)). The mean nocturnal F_{cb} was lowest in March and highest in August (0.5 and $3.0 \mu\text{mol m}^{-2} \text{ s}^{-1}$, respectively). The July 1996 trace showed a large mid-day depression, where fluxes approached a minimum of $0.5 \mu\text{mol m}^{-2} \text{ s}^{-1}$ at 1100 h, suggesting that photosynthesis below the sensor height influenced the measurements. The diurnal pattern contrasts with those we

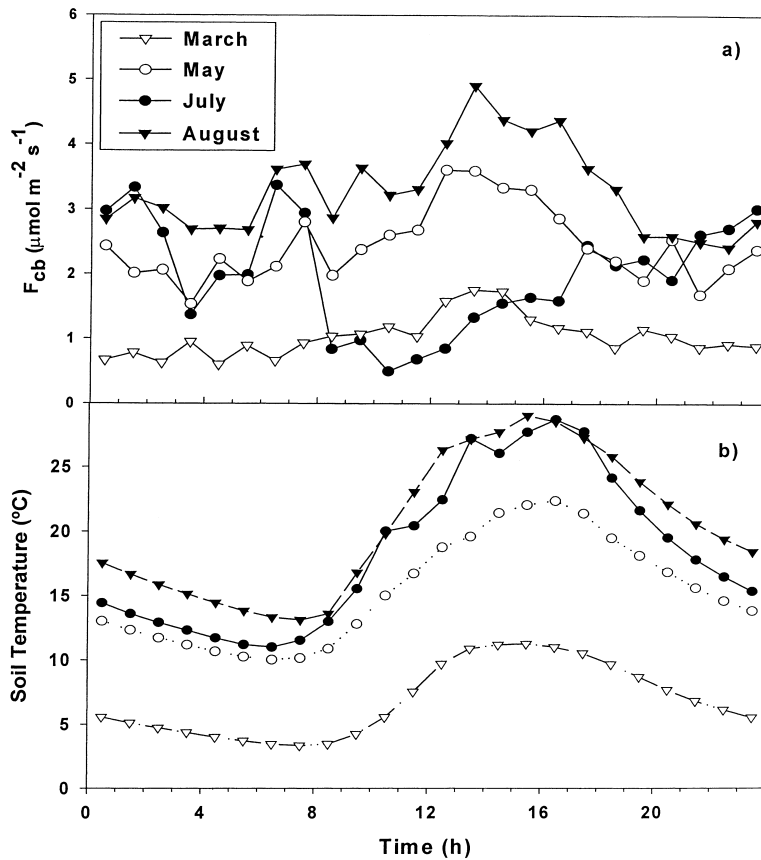


Fig. 1. (a) Seasonal variation in diel below-canopy eddy covariance measurements of CO₂ fluxes (F_{cb}). Hourly values were calculated from the hourly means for groups of days in each month; March (Days 78–89, 1997), May (Days 129–151, 1997), July (Days 187–205, 1996), and August (Days 220–234, 1997). (b) Seasonal variation in soil temperature ($^{\circ}\text{C}$) at 4 cm depth.

have measured under denser conifer and deciduous forest canopies. In those studies we observed that maximal rates of soil/root respiration occurred during midday because understory photosynthesis was negligible (Baldocchi and Vogel, 1996).

We then examined the relation between hourly soil temperature at different depths (2, 4, 8, 15 cm, and air temperature at 1 m) and F_{cb} . Model parameters were determined from the log-transformed equation ($\ln(F_{cb}) = \ln(b_0) + b_1 \cdot T_s$) and a linear least-squares regression model (S-PLUS, Mathsoft, Seattle, WA), because of uneven distribution of the error terms with season. The temperature response models that fit best used soil temperature at 4 cm depth, as determined from the March, May and August 1997 data ($r^2 = 0.38$; $Q_{10} = 1.9$) and the March and May data only ($r^2 = 0.43$; $Q_{10} = 2.2$; Fig. 2).

3.3. Chamber measurements

3.3.1. Soil surface CO₂ efflux

On 4 days in July 1996, F_s measured in the morning ranged from 1.0 to 6.5 $\mu\text{mol m}^{-2} \text{s}^{-1}$ at the 45 points across the site. About 70% of the measurements ranged between 2.0 and 3.0 $\mu\text{mol m}^{-2} \text{s}^{-1}$ on all 4 days (Fig. 3). There was a moderate variation in F_s across the site, except for a few extreme values.

Fig. 4 shows how F_s changed through the year. Seasonally, F_s increased from a winter low of 0.5 $\mu\text{mol m}^{-2} \text{s}^{-1}$ (SE = 0.06) to a peak in late May of 5.8 $\mu\text{mol m}^{-2} \text{s}^{-1}$ (SE = 0.55) and averaged 2.5 $\mu\text{mol m}^{-2} \text{s}^{-1}$ (SE = 0.15) through July and August. There was a slight increase again in September before the winter decline in F_s . Pre-dawn leaf water potential followed similar seasonal trends

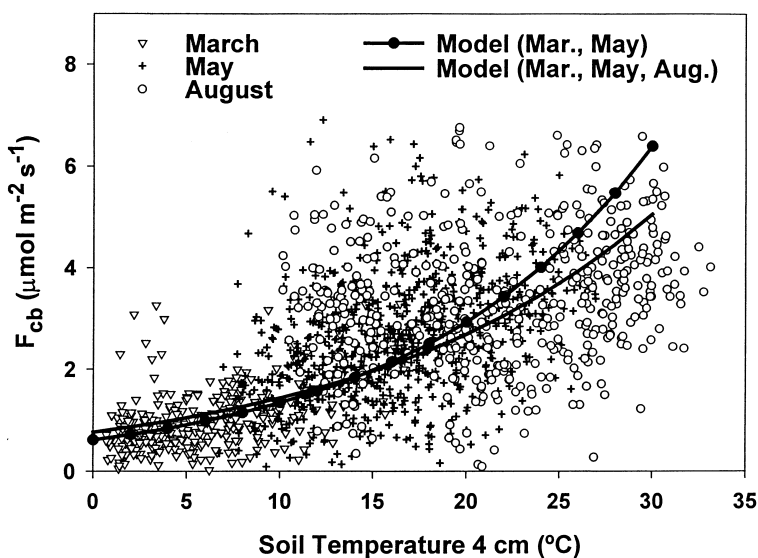


Fig. 2. The relationship between below-canopy CO_2 flux (F_{cb}) and soil temperature at 4 cm depth (T_{s4}). Two regression lines are shown. One is for March and May 1997 data only ($\ln(F_{cb}) = \ln(0.62) + 0.078 T_{s4}$; $r^2 = 0.43$, $n = 1135$, $Q_{10} = 2.2$), and the other includes data for March, May and August 1997 ($\ln(F_{cb}) = \ln(0.76) + 0.063 T_{s4}$; $r^2 = 0.38$, $n = 1593$, $Q_{10} = 1.9$).

(Fig. 4). Our data showed maximum water stress (lowest Ψ_{predawn}) in August (-1.10 MPa) and little water stress in May and September. The days of low water stress coincided with seasonal precipitation (Fig. 4). When Ψ_{predawn} and F_s were averaged in 10 day classes, linear regression showed that Ψ_{predawn}

during the growing season explained 54% of the variation in F_s ($F_s = 4.14 + 2.00 \Psi_{\text{predawn}}$).

Various statistical models were fitted to the soil CO_2 flux and environmental data (Table 3). The model with the best fit took into account soil temperature (15 cm depth), the C : N ratio of litter, and soil water content at 0–100 cm depth (Eq. (2) in Table 3; RSE = 0.539). We conducted an F -test to compare the simple temperature response model ($F_s = 1.216 \exp(0.059 T_s)$, Eq. (1) in Table 3) with the model with the best fit and found no significant difference ($F = 1.8$; Motulsky and Ransnas, 1987). Thus, soil temperature accounted for most of the variation in F_s . The Q_{10} for the simple temperature–response equation was 1.8, close to the Q_{10} 1.9 estimated for F_{cb} in March, May and August (Fig. 2). It is also within the range reported by Raich and Schlesinger (1992) and close to the value (1.9) found by Arneeth et al. (1998) in sandy soils of a *P. radiata* stand in New Zealand. Other variables that we tested in statistical empirical models (e.g. nitrogen content of litter, humus and soil, and soil water content at 0–30 cm depth) did not improve correlations with F_s .

Fig. 5 shows the simple temperature–response curve with the curve for a predictive equation proposed by Lloyd and Taylor (1994) from their analysis

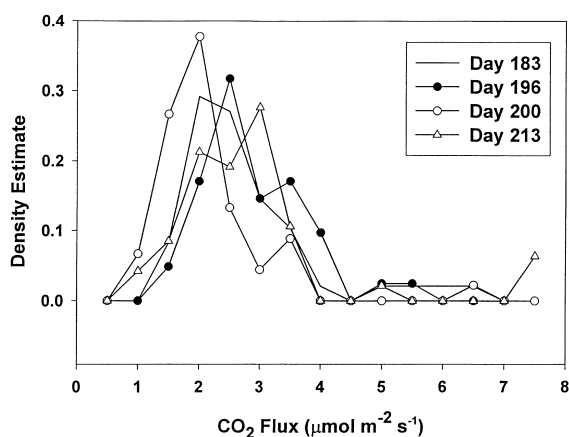


Fig. 3. Probability density function of soil CO_2 efflux measurements (F_s) across the site on 4 days in July 1996. A moderate amount of variation in F_s was observed across the site, except for a few extreme values.

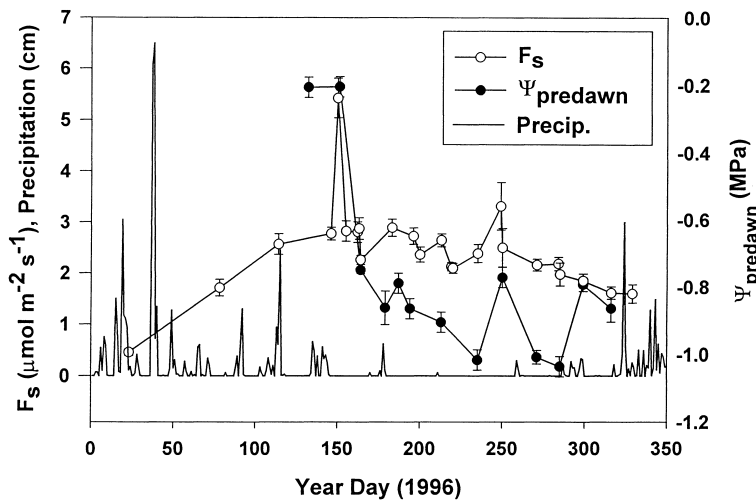


Fig. 4. Mean of soil CO₂ efflux (F_s) calculated from measurements on 25 days through the year, mean pre-dawn leaf water potential (Ψ_{predawn} in MPa), and precipitation (cm).

of datasets from several ecosystems. Their equation appears to fit the upper boundary of our data. When we fit their model to our data, assuming the same temperature constant (308.56 K), our fitted regression coefficient (213.17 K; Equation 4 in Table 3) was slightly lower than the value they observed (227.13 K). In their study, the equation provided accurate estimates of soil CO₂ flux across a wide range of soil temperatures and ecosystem-types without soil moisture deficits. The water limitation at our pine site could partly explain the discrepancy with our results.

The F_s model proposed by Norman et al. (1992), used by Arneth et al. (1998), and similar to Hanson et al. (1993) (equation 5 in Table 3) had a higher RSE (1.73) than the rest of the models that we tested (Table 3). The regression coefficient ($\beta = 0.059$) corresponds with a Q_{10} of 1.8, the same value as the simple temperature response model.

We evaluated the effect of the depth at which soil temperature measurements are made on the simple temperature–response model ($F_s = b_0 \exp(b_1 \cdot T_s)$) using F_s measurements taken next to the temperature profile system in an old stand. Soil temperature at 2 cm

Table 3
Selected statistical models for estimating soil CO₂ flux from environmental variables

Model		Residual standard error
1	$F_s = 1.216 \times \exp(0.059 \times T_s)$	0.544
2	$F_s = (0.014 \times \text{CN}_1) + (-2.227 \times \theta_{100}) + \exp(0.064 \times T_s)$	**0.539
3	$F_s = 0.964 + (0.229 \times T_s) - (0.148 \times \theta_{100}) - (0.005 \times T_s^2) - (5.04 \times \theta_{100}^2)$	0.555
4	$F_s = 2.19 \times \exp(308.56 \times ((1/(283.15 - 213.17)) - 1/(T_s + 273.15 - 213.17)))$	0.609
5	$F_s = 8.8 \times (\theta - \theta_{\min})/(\theta_{\max} - \theta_{\min}) \exp(0.059 \times (T_s - 18))$	1.731

Equations are based on data gathered all year at young, old and mixed-age stands ($n = 9$ plots). The model with the lowest residual standard error is identified with a double asterisk. T_s is soil temperature (°C) at 15 cm depth near the chamber, CN_1 is the carbon : nitrogen ratio for litter, θ_{100} is soil water content at 0–100 cm. Equation 4 is from Lloyd and Taylor (1994, Equation 11), where 2.19 is soil surface CO₂ efflux at our site at 10°C (determined from $F_s = 1.216 \times \exp(0.059 \times T_s)$), 308.56 is a temperature constant (K), and 213.17 (K) is the fitted regression coefficient. Equation 5 proposed by Norman et al. (1992), used by Arneth et al. (1998), and similar to Hanson et al. (1993): $F_s = F_{s\text{max}} \times (\theta - \theta_{\min})/(\theta_{\max} - \theta_{\min}) \exp(\beta \times (T_{s15} - T_{s\text{max}}))$, where $F_{s\text{max}}$ is the maximum flux measured at the maximum soil temperature ($T_{s\text{max}}$) at 15 cm depth, T_{s15} is soil temperature at 15 cm depth (°C), β is the fitted coefficient.

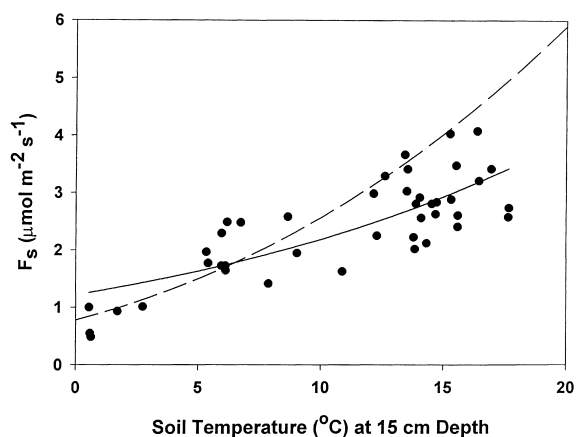


Fig. 5. Soil CO₂ flux (F_s) versus soil temperature at 15 cm depth (°C), from plot means for old, young and mixed stands that were measured with chambers through 1996. Each data point represents the mean of 3 subplots per stand. The fitted equation (solid line, —), is the one listed first in Table 3 ($F_s = b_0 \exp(b_1 T_s)$), $r^2 = 0.60$, $Q_{10} = 1.8$). The dashed (---) line is F_s predicted from Eq. (3) in Table 3 (Lloyd and Taylor (1994)).

resulted in the model with the best fit (RSE = 0.526). The RSE varied slightly, from 0.526 to 0.603 for different depths. We also tested the use of mean soil temperatures from 2 to 8 cm, 2 to 16 cm, and 2 to 32 cm depth in the temperature–response model, hypothesizing that a depth-integrated soil temperature would incorporate distribution of the physical and biotic environments through the active soil profile. The use of mean soil temperature for the profiles did not improve the model fit.

3.4. Chamber–eddy flux comparison

In July 1996, photosynthesis of nearby trees and ground vegetation could have offset some soil CO₂ flux and thus account for the decrease in F_c measured by the below-canopy flux system. The openness of the forest canopy allowed a sufficient amount of light to penetrate to the understory to sustain photosynthesis. The 20-day mean hourly PAR at 1.0 m height reached a maximum of $262 \mu\text{mol m}^{-2} \text{s}^{-1}$ and VPD at 2 m height reached a maximum of 3.1 kPa in the afternoon. From LAI profile calculations (Law et al. in prep.), we estimated that about $0.08 \text{ m}^2 \text{ m}^{-2}$ of the total LAI of *P. ponderosa* was below the F_{cb} measurement height (2 m). The hourly PAR at 1.0 m and VPD at 2.0 m

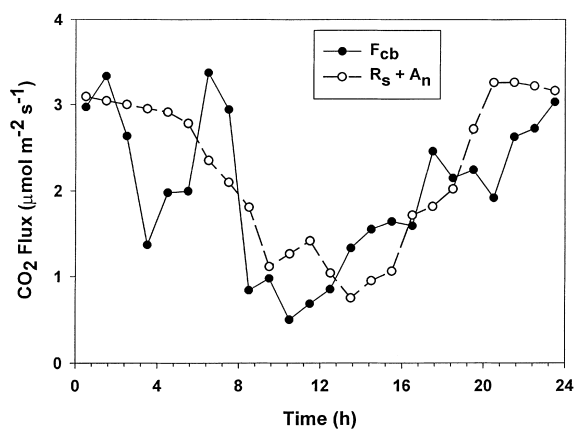


Fig. 6. Comparison of mean eddy covariance below-canopy CO₂ fluxes (F_{cb}) in July 1996 and chamber estimates of F_{cb} ($R_s + A_n$) calculated from Eq. (2).

were used with the fitted light-response models for *P. ponderosa* and *F. vesca* to estimate hourly net assimilation for the 20 days that F_{cb} measurements were made in July 1996. The maximum net assimilation of vegetation below the F_{cb} measurement height was reached by mid-morning ($1.4 \mu\text{mol m}^{-2} \text{ ground s}^{-1}$). Fig. 6 shows the chamber estimates of the 20-day mean hourly below-canopy CO₂ fluxes (Eq. (2)) compared with mean hourly F_{cb} measurements. The figure suggests that photosynthesis of the understory and the lower canopy of young trees could account for the mid-day depression in F_{cb} observed in July. Although we did not see the same trend in F_{cb} in August 1997, our phenology records show that senescence began earlier in 1997 than in 1996. *F. vesca* was senescing in August 1997, and $\sim 1/3$ of the pine foliage had senesced by Day 215.

We used probability density functions to compare distributions of F_{cb} and F_s observations over selected periods in Fig. 7 because of spatial and temporal differences in measurement methods. In August 1997, we measured F_s at approximately 2 h intervals over 4 days and nights (Days 224–228) at three plots within 30 m of the F_{cb} measurements. We separated the August data into diurnal (Fig. 7(a)) and nocturnal (Fig. 7(b)) datasets. The probability density functions and means were very similar for nocturnal and diurnal F_s (means 2.6 ± 0.08 and $2.8 \pm 0.06 \mu\text{mol m}^{-2} \text{ s}^{-1}$, respectively). The mean nocturnal F_{cb} in August was $3.5 \pm 0.28 \mu\text{mol m}^{-2} \text{ s}^{-1}$, significantly greater than

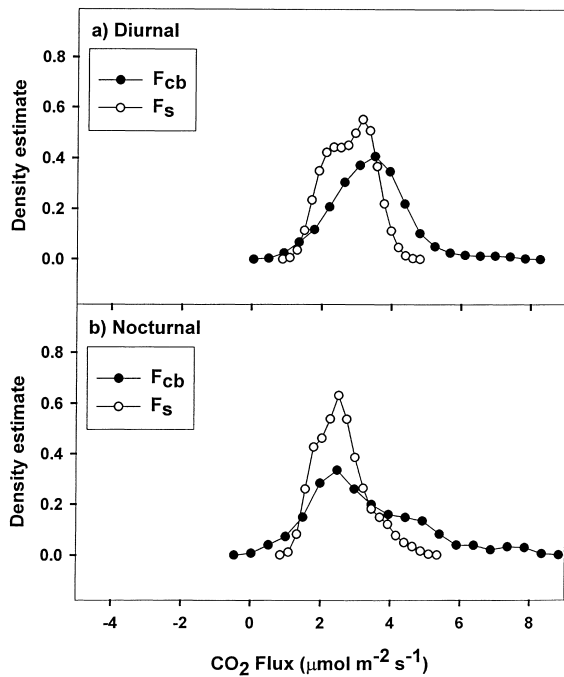


Fig. 7. Comparison of probability density functions for soil CO_2 efflux (F_s) and below-canopy eddy covariance measurements (F_{cb}). (a) August 1997 nocturnal F_s and F_{cb} (Days 224–228), and (b) August 1997 diurnal F_s and F_{cb} .

F_s (Welch modified two-sample t -test, $p = 0.005$). Daytime F_{cb} ($3.4 \pm 0.12 \mu\text{mol m}^{-2} \text{s}^{-1}$) was also significantly greater than F_s ($p = 0.0005$). There was more variation in the F_{cb} measurements, particularly at night when friction velocity, u_* , was typically low and the wind was from the south (Fig. 8). There was no correlation between F_{cb} and u_* , nor between F_s and u_* (Fig. 9), contrary to findings by Arneeth et al. (1998) who used u_* along with soil moisture and temperature to predict F_s . A comparison of the nightly mean F_{cb} and the whole ecosystem respiration calculated from chamber measurements on soils, foliage and wood showed that on three of the four nights in August, the mean F_{cb} was almost the same as ecosystem respiration (Fig. 10).

For the same four nights in August 1997, the mean nocturnal NEE ($F_{ca} + F_{stor}$), was $2.8 \pm 0.40 \mu\text{mol m}^{-2} \text{s}^{-1}$, between F_{cb} ($3.5 \pm 0.28 \mu\text{mol m}^{-2} \text{s}^{-1}$) and F_s ($2.6 \mu\text{mol m}^{-2} \text{s}^{-1}$). The mean nocturnal $F_{ca} + F_{stor}$ was significantly lower than ecosystem respiration from chamber data, and even F_{cb} and F_s

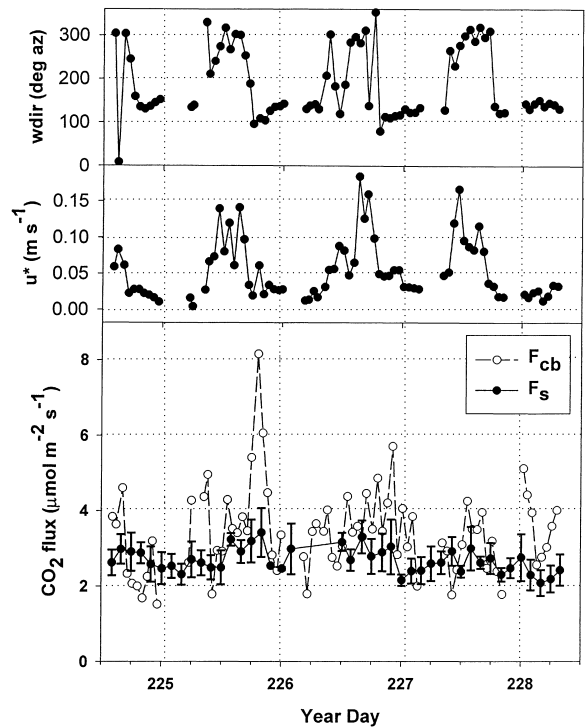


Fig. 8. Wind direction (wdir, 90° is east), below-canopy friction velocity (u_* , m s^{-1}), soil CO_2 efflux measurements (F_s) and below-canopy eddy covariance measurements (F_{cb}) in August 1997. The F_s data are means (vertical bars represent standard errors) of observations at 3 locations within the footprint of the F_{cb} measurements, which were averaged hourly. Days on the x -axis are midnight. Gaps in the data were the result of removal in the screening process.

alone on Day 227, which was more turbulent (mean above-canopy $u_* = 0.30 \text{ m s}^{-1}$) than the other three nights ($u_* < 0.15 \text{ m s}^{-1}$; Fig. 10).

4. Discussion

In our evaluation of models for estimating F_s , soil temperature appears to have the most influence. Other studies had similar results (Singh and Gupta, 1977; Weber, 1985; Raich and Schlesinger, 1992; Suarez and Šimunek, 1993). Microbial and root activity have been correlated with soil temperature. Decomposition rates are very low below 0°C soil temperature, increase rapidly from 10 to 30°C , then decrease again when temperature exceeds 40°C (Agren et al., 1991). Root

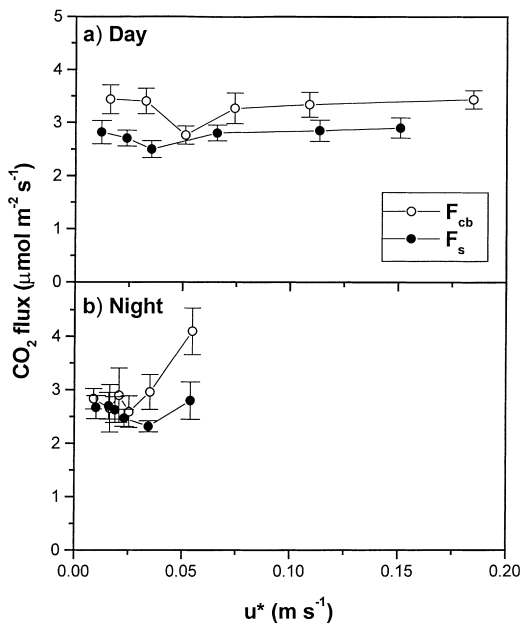


Fig. 9. The relation between soil CO₂ efflux measurements (F_s) and below-canopy friction velocity (u^*) and eddy covariance measurements (F_{cb}) and u^* on 4 days in August 1997 (a) during daylight hours and (b) at night. Points are means and standard errors. Data were sorted by u^* , with each interval during the night containing 10 observations of F_s and 8 observations of F_{cb} , and each interval during the day containing 12 observations of F_s and 15 observations of F_{cb} .

respiration includes the costs of maintaining living cells and has been modeled as an exponential function of temperature (Penning de Vries, 1975; Ryan, 1991). The Q_{10} of our F_s temperature–response Equation (1.8) is similar to that for the F_{cb} temperature–response equation and it is within the range of values reported in the literature; the median Q_{10} of numerous studies is 2.4, with a bimodal distribution peaking at 1.9 and 2.5 (Raich and Schlesinger, 1992). When Q_{10} values are calculated from data spanning the seasons, they are influenced by respiration costs of root production, including growth-related maintenance respiration, suggesting that it is important to develop seasonal temperature–response equations. Limited datasets and small temperature ranges within season often preclude this approach, but the use of measurements by automated chamber systems or below-canopy eddy covariance, accounting for understory contributions, would provide a large amount of temporal data that includes diel variations in temperature.

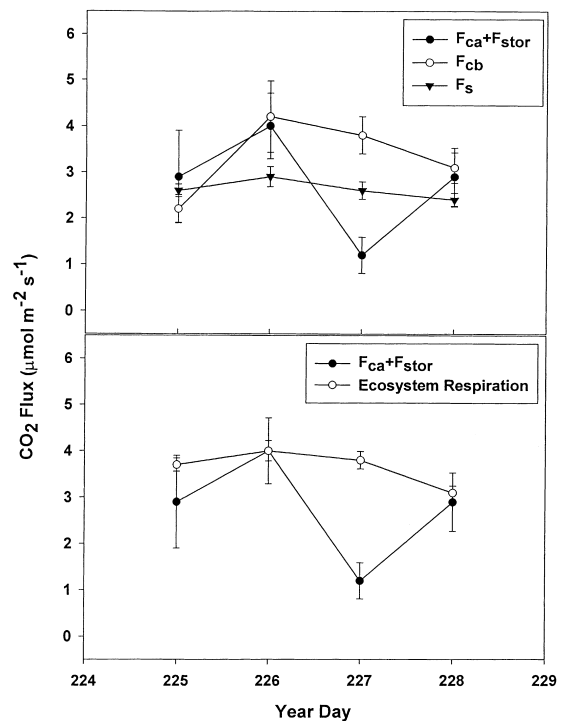


Fig. 10. Mean nightly net ecosystem exchange ($F_{ca} + F_{stor}$), below-canopy CO₂ fluxes (F_{cb}), soil CO₂ effluxes (F_s), and ecosystem respiration from scaled-up chamber measurements on soils, foliage and wood on four nights in August, 1997.

The reasonable correlation we found between F_s and $\Psi_{predawn}$ suggests that $\Psi_{predawn}$ is a better indicator of soil water availability to autotrophs and heterotrophs during the growing season than is soil water content at the depths we sampled. Davidson et al. (1998) found that a seasonal decline in F_s in a mixed hardwood forest was correlated exponentially with decreasing soil matric potential, a component of soil water potential, indicating the effect of drought stress. Microbial activity generally decreases with soil water potential (Orchard et al., 1992). Fogel and Cromack (1977) found that in Douglas-fir in Oregon, $\Psi_{predawn}$ and soil moisture at 0–5 cm depth were good predictors of needle decomposition ($r^2 = 0.92$ and 0.91, respectively).

Substrate quality influences decomposition rates, which in turn influence soil CO₂ efflux. A high C : N ratio of litter suggests that decomposition will proceed slowly. The average C : N of litter in the young stands (50) was slightly higher than the old stands (46;

Table 1). A repeated measures test showed that F_s was significantly higher in young stands than in old stands ($p = 0.08$ for 10 stands over 23 days; Law et al., 1999). The C : N ratio in litter did not explain much of the variation in F_s , and it may not have varied enough within the site to make a discernible difference (Table 1). A better index of decomposition rates that could be evaluated as a variable for estimating F_s is the lignin content of soil or the lignin : nitrogen ratio (Melillo et al., 1982). Fogel and Cromack (1977) found that lignin was a better predictor of litter decomposition than was the C : N ratio of litter. We did not have lignin data to include in the model evaluations.

The spatial variation in chamber measurements of soil CO_2 efflux across the site on a given day was relatively small (Figs. 3 and 4), with only a few extreme values. We suspected the high F_s values were due to a high concentration of roots, mycorrhizae or microbial activity below the chamber. The use of chambers that cover a very small surface area of the soil contributes to difficulty of obtaining consistent results. The approximate accuracy of the sample mean achieved with a 0.10 level of significance averaged within $\pm 12\%$ of the true site mean ($n = 45$, accuracy $\cong cv \times t_{0.10}/\sqrt{n}$; Eckblad, 1991). Over 25 days of measurements, the mean F_s was $2.8 \mu\text{mol m}^{-2} \text{s}^{-1}$ in the young stands and $2.3 \mu\text{mol m}^{-2} \text{s}^{-1}$ in the old stands. Although the difference between these values was statistically significant ($p = 0.08$), it is smaller than within-site differences in F_s at other sites. For example, in a deciduous forest in Massachusetts, Goulden et al. (1996) found mean rates of $3.8 \mu\text{mol m}^{-2} \text{s}^{-1}$ in a poorly drained area and $7.5 \mu\text{mol m}^{-2} \text{s}^{-1}$ in an upland area of their site.

Absolute rates of F_s at our site were also low (e.g. nocturnal mean $2.6 \mu\text{mol m}^{-2} \text{s}^{-1}$ in August 1997) compared with the temperate deciduous forest (nocturnal mean $4.5 \mu\text{mol m}^{-2} \text{s}^{-1}$; Goulden et al., 1996). In boreal jack pine forests (*P. banksiana*), which are northern latitude forests on coarse-textured soils, nocturnal F_s values of $\sim 2 \mu\text{mol m}^{-2} \text{s}^{-1}$ have been reported for May–September (Lavigne et al., 1997), comparable to values at our site. Our low winter values of F_s ($0.5 \mu\text{mol m}^{-2} \text{s}^{-1}$) are also similar to those observed in boreal forests (Rayment and Jarvis, 1997), and in a young irrigated pine stand in

Massachusetts ($0.1 \mu\text{mol m}^{-2} \text{s}^{-1}$; Raich and Potter, 1995).

Seasonal increase in F_{cb} from March to May and August 1997 can be explained primarily by the influence of increased temperatures on respiration. Seasonal differences in root activity could strongly influence F_s and F_{cb} . Fine root production is generally high in the spring and fall (Vogt et al., 1986). Using ^{14}C labeling, Smith and Paul (1988) found that carbon allocation to *P. ponderosa* roots peaked in spring and fall, coinciding with periods of root growth. Likewise, coarse root respiration by *P. sylvestris* peaked in autumn when soil temperatures remained warm (Linder and Troeng, 1981). On the other hand, there is typically little root growth during periods of rapid shoot growth on the trees (June and July at our site; Eissenstat and Van Rees, 1994). Our measured F_s rates reached maxima in May and September 1996, and the increase may have coincided with carbon allocation to roots (Raich and Nadelhoffer, 1989). Autotrophs and heterotrophs should benefit most when temperatures are higher and water is available, as in late May and September 1996. The F_s rates were generally lower mid-June through August 1996, increasing temporally following rain events. The decreased soil moisture in July and August may counteract benefits from increased soil temperature (Davidson et al., 1998).

Below-canopy eddy covariance measurements can include the influence of photosynthesis and respiration by vegetation below the sensor height. In our other studies on temperate deciduous forests, photosynthesis had no obvious influence on F_{cb} measurements using the same flux system (Baldocchi and Vogel, 1996). Norman et al. (1997), however, found that even though photosynthesis was not obvious in F_{cb} measurements in a jack pine forest, there was a better correlation between F_s and F_{cb} when they adjusted F_{cb} for photosynthesis by understory growing around the eddy covariance system. It appeared that photosynthesis had a significant influence on F_{cb} in July 1996 (Figs. 1 and 6), but little influence in May and August 1997. Our seasonal phenology records indicate that strawberry and bracken fern had just started to appear mid-to-late May, but had senesced by mid-September. Needle senescence began earlier than normal in August 1997, probably because of the low cumulative rainfall that year. Also, the daytime mean F_s was higher in August 1997 than in July 1996. More

photosynthesis and less soil CO₂ flux in July 1996 than in August 1997 suggests that the balance between photosynthesis and respiration was different enough to account for the observed differences in diurnal F_{cb} .

The broader distribution of F_{cb} data compared with F_s data (Fig. 7) shows that F_{cb} data were more variable. Greater variation in measured fluxes can be expected on calm nights (e.g. $u_* < 0.25 \text{ m s}^{-1}$; Goulden et al., 1996; Lavigne et al., 1997) and when the source area of the fluxes changes with turbulence and wind direction (Baldocchi, 1997). The poor correlation between F_{cb} and u_* in August (Figs. 2 and 9) suggests that the large variations in F_{cb} are due to other factors. Analysis of error in F_{cb} measurements indicates a systematic error of $\pm 12\%$, largely from CO₂ calibration uncertainties (5–10% difference in calibration coefficients from one calibration to the next).

Since below-canopy fluxes are typically intermittent, sampling error is likely to be large. Errors in estimated means and variances of fluxes can be reduced by increasing the size of datasets. Thus the effect of random errors can be minimized by examining the convergence of calculations of net fluxes with increasing size of datasets (Wyngaard, 1974; Moncrieff et al., 1996). This is our reason for bin-averaging F_{cb} by the hour and averaging hourly fluxes over several days. With these approaches, the random errors tend to converge, but systematic errors remain (Moncrieff et al., 1996).

The below-canopy flux measurements represent the integrated contributions of variations in soils, understory cover, sapwood, and the lower portion of young tree canopies in a source area upwind of the measurement system. The area of influence changes with atmospheric stability and wind speed. Open forest canopies that do not significantly attenuate horizontal wind speed and/or atmospheric conditions that dampen turbulent fluctuations will extend the flux footprint. Consequently, stable nocturnal atmospheric conditions will result in a larger footprint. The footprint of the above-canopy flux system is generally larger than the below-canopy flux system. For evaluating contributions of soils to net ecosystem exchange of CO₂ measured with above-canopy flux systems, it is important to ensure that the footprints of both flux systems have source regions with similar characteristics. Chamber measurements covering a large por-

tion of the above-canopy flux footprint can be used to determine spatial variability in the soil fluxes.

In evaluating nocturnal fluxes measurements, there was reasonable agreement between $F_{ca} + F_{stor}$ and ecosystem respiration from chamber data on calm nights (above-canopy $u_* \sim 0.15 \text{ m s}^{-1}$; Fig. 10), contrary to other studies where CO₂ was found to 'escape' by an undetected route under these conditions (Goulden et al., 1996). On the more turbulent night (above-canopy $u_* = 0.30 \text{ m s}^{-1}$, Day 227), $F_{ca} + F_{stor}$ was significantly lower than ecosystem respiration and even lower than F_{cb} and F_s . Our hypothesis is that under calm conditions (e.g. $u_* < 0.15 \text{ m s}^{-1}$ as observed on three of the nights), F_{ca} is negligible and has no impact on the CO₂ budget. In this case, any missed flux by the above-canopy eddy correlation system is of no consequence. Under weak wind conditions (e.g. $u_* = 0.30 \text{ m s}^{-1}$), F_{ca} begins to become significant and fluxes missed by the above-canopy eddy correlation system degrade the CO₂ budget. Under windy conditions, the above-canopy eddy correlation measurement is a good approximation and the CO₂ budget improves again.

5. Conclusions

The combination of chamber and below-canopy eddy covariance methods for studying soil CO₂ efflux has several benefits. Chamber measurements of F_s at several locations across the site provide good estimates of spatial variation in soil CO₂ efflux, while eddy covariance measurements of below-canopy fluxes provide the temporal resolution necessary for characterizing diel and seasonal changes. Chamber measurements may help to distinguish different sources of below-canopy fluxes, and associated micrometeorological measurements can identify processes that may be neglected by use of chambers alone (e.g. photosynthesis by the understory).

Soil processes have a major influence on carbon exchange between open-canopy forests and the atmosphere. Accurate measurements of soil contributions to net ecosystem exchange of carbon are necessary when estimating seasonal and annual carbon budgets of terrestrial ecosystems. This study emphasizes the need for better modeling of soil CO₂ transport and production in carbon balance models, and for contin-

uous measurement of below-canopy fluxes along with above-canopy fluxes to better quantify the seasonal and annual contribution of soils to the carbon budget.

Acknowledgements

This study was funded by NASA (grant #NAGW-4436). We are grateful to Steve Van Tuyl, Will Hutchinson, and Mike Unsworth for their field assistance. Thanks to John Norman, Rick Garcia and Mike Ryan for their helpful suggestions on soil chamber design and measurements. We thank Larry Mahrt for his helpful comments on nocturnal fluxes, Mike Unsworth for his review of the manuscript, and Laurel Grove for her editorial comments. We gratefully acknowledge the assistance of the Sisters Ranger District and Sarah Greene of the U.S. Forest Service in establishing the study site. The study site is located in a Research Natural Area; such areas are selected to represent different vegetation-types in their natural condition.

Appendix

Symbols

A_n	net assimilation of carbon ($\mu\text{mol m}^{-2}$ half-surface area of needles s^{-1})
A_{max}	maximum assimilation rate
α_p	quantum efficiency of photosynthesis
β	exponent in temperature response equations for CO_2 flux density ($\ln Q_{10}/10$)
F_{cb}	CO_2 flux density measured below the canopy by the eddy covariance method ($\mu\text{mol m}^{-2} \text{s}^{-1}$)
F_f	CO_2 flux density for foliage ($\mu\text{mol m}^{-2} \text{s}^{-1}$)
F_s	CO_2 flux density for soils measured with chambers ($\mu\text{mol m}^{-2} \text{s}^{-1}$)
F_{smax}	maximum flux density of CO_2 for soils measured at the maximum soil temperature ($\mu\text{mol m}^{-2} \text{s}^{-1}$)
F_w	CO_2 flux density for wood biomass in live trees ($\mu\text{mol m}^{-2} \text{s}^{-1}$)
HSA	half-surface area of leaves, half the total surface area (m^2)
LAI	leaf area index (m^2 leaf half-surface area m^{-2} ground)

LE	latent heat flux (W m^{-2})
Ψ_{predawn}	predawn leaf water potential (MPa)
PAR	photosynthetically active radiation (400–700 nm; $\mu\text{mol m}^{-2} \text{s}^{-1}$)
Q_{10}	rate of change in CO_2 flux with a 10°C change in temperature ($\exp(\beta \cdot 10)$)
R_s	respiration ($\mu\text{mol m}^{-2} \text{s}^{-1}$)
RSE	residual standard error
θ_i	soil water content ($\text{m}^3 \text{m}^{-3}$) at depth i (cm)
θ_{min}	minimum soil water content measured at 0–30 cm depth ($\text{m}^3 \text{m}^{-3}$)
θ_{max}	maximum soil water that can be held against gravity ($\text{m}^3 \text{m}^{-3}$)
T_{si}	soil temperature ($^\circ\text{C}$) at depth i (cm)
T_{smax}	maximum soil temperature observed at 15 cm depth ($^\circ\text{C}$)
u^*	friction velocity (m s^{-1}), a measure of turbulence
VDP	vapor pressure deficit (kPa)
wdir	wind direction (degrees azimuth; 90° is east)

References

- Agren, G.L., McMurtrie, R.E., Parton, W.J., Pastor, J., Shugart, H.H., 1991. State-of-the-art of models of production–decomposition linkages in conifer and grassland ecosystems. *Ecol. Applic.* 1, 49–53.
- Anthoni, P.M., Law, B.E., Unsworth, M.H., 1999. Carbon and water vapor exchange of an open-canopied ponderosa pine ecosystem. *Agric. For. Meteorol.*, in press.
- Arnth, A., Kelliher, F.M., Gower, S.T., Scott, N.A., Byers, J.N., McSeveny, T.M., 1998. Environmental variables regulating soil carbon dioxide efflux following clear-cutting of a *Pinus radiata* D Don plantation. *J. Geophys. Res.* 103, 5695–5707.
- Auble, D.L., Meyers, T.P., 1992. An open path, fast response infrared absorption gas analyzer for H_2O and CO_2 . *Boundary Layer Meteorol.* 59, 243–256.
- Baldocchi, D.D., 1997. Flux footprints within and over forest canopies. *Boundary Layer Meteorol.* 85, 273–292.
- Baldocchi, D.D., Hicks, B.B., Meyers, T.P., 1988. Measuring biosphere–atmosphere exchanges of biologically related gases with micrometeorological methods. *Ecology* 69, 1331–1340.
- Baldocchi, D.D., Vogel, C.A., 1996. Energy and CO_2 flux densities above and below a temperate broad-leaved forest and a boreal pine forest. *Tree Physiol.* 16, 5–16.
- Black, T.A., Hartog, G., Neumann, H.H., Blanken, P.D., Yang, P.C., Russell, C., Nestic, Z., Lee, X., Chen, S.G., Staebler, R., Novak, M.D., 1996. Annual cycles of water vapour and carbon dioxide

- fluxes in and above a boreal aspen forest. *Global Change Biol.* 2, 219–230.
- Bowden, R.D., Nadelhoffer, K.J., Boone, R.D., Melillo, J.M., Garrison, J.B., 1993. Contributions of aboveground litter, belowground litter, and root respiration to total soil respiration in a temperate mixed hardwood forest. *Can. J. For. Res.* 23, 1402–1407.
- Burton, A.J., Zogg, G.P., Pregitzer, K.S., Zak, D.R., 1998. Drought reduces root respiration in sugar maple forests. *Ecol. Appl.*, in press.
- Davidson, E.A., Belk, E., Boone, R.D., 1998. Soil water content and temperature as independent or confounded factors controlling soil respiration in a temperate mixed hardwood forest. *Global Change Biol.* 4, 217–227.
- Eckblad, J.W., 1991. How many samples should be taken? *BioScience* 41, 346–348.
- Edwards, N.T., Sollins, P., 1973. Continuous measurement of carbon dioxide evolution from partitioned forest floor components. *Ecology* 54, 406–412.
- Eissenstat, D.M., Van Rees, K.C.J., 1994. The growth and function of pine roots. *Ecol. Bull.* 43, 76–91.
- Fang, C., Moncrieff, J.B., 1998. An open-top chamber for measuring soil respiration and the influence of pressure differences on CO₂ efflux measurement. *Functional Ecol.* 12, 319–330.
- Fogel, R., Cromack, K., 1977. Effect of habitat and substrate quality on Douglas fir litter decomposition in western Oregon. *Can. J. Bot.* 55, 1632–1640.
- Goulden, M.L., Munger, J.W., Fan, S.-M., Daube, B.C., Wofsy, S.C., 1996. Measurements of carbon sequestration by long-term eddy covariance: Methods and a critical evaluation of accuracy. *Global Change Biol.* 2, 169–182.
- Hanson, P.J., Wullschlegel, S.D., Bohlman, S.A., Todd, D.E., 1993. Seasonal and topographic patterns of forest floor CO₂ efflux from an upland oak forest. *Tree Physiol.* 13, 1–15.
- Knight, D.H., Vose, J.M., Baldwin, V.C., Ewel, K.C., Grodzinska, K., 1994. Contrasting patterns in pine forest ecosystems. *Ecol. Bull.* 43, 9–19.
- Koide, R.T., Robichaux, R.H., Morse, S.R., Smith, C.M., 1991. Plant water status, hydraulic resistance and capacitance. In: Percy, R.W., Ehleringer, J., Mooney, H.A., Rundel, P.W. (Eds.), *Plant Physiological Ecology: Field Methods and Instrumentation*, Chapman and Hall, London, pp. 161–183.
- Landsberg, J.J., 1986. *Physiological Ecology of Forest Production*, Academic Press, London, 198pp.
- Lavigne, M.B., Ryan, M.G., Anderson, D.E., Baldocchi, D.D., Crill, P.M., Fitzjarrald, D.R., Goulden, M.L., Gower, S.T., Massheder, J.M., McCaughey, J.H., Rayment, M., Striegl, R.G., 1997. Comparing nocturnal eddy covariance measurements to estimates of ecosystem respiration made by scaling chamber measurements at six coniferous boreal sites. *J. Geophys. Res.* 102, 28977–28985.
- Law, B.E., 1995. Estimation of leaf area index and light intercepted by shrubs from digital videography. *Remote Sens. Environ.* 51, 276–280.
- Law, B.E., Ryan, M.G., Anthoni, P.M., 1999. Seasonal and annual respiration of a ponderosa pine ecosystem. *Global Change Biol.*, in press.
- Law, B.E., Waring, R.H., 1994. Combining remote sensing and climatic data to estimate net primary production across Oregon. *Ecol. Appl.* 4, 717–728.
- Linder, S., Troeng, E., 1981. The seasonal variation in stem and coarse root respiration of a 20-year-old Scots pine (*Pinus sylvestris* L.). *Mittl. Forst. Bundesvers.* 142, 125–139.
- Lloyd, J., Taylor, J.A., 1994. On the temperature dependence of soil respiration. *Functional Ecol.* 8, 315–323.
- Melillo, J.D., Aber, J., Muratore, J.F., 1982. Nitrogen and lignin control of hardwood leaf litter decomposition dynamics. *Ecology* 63, 621–626.
- Moncrieff, J.B., Mahli, Y., Leuning, R., 1996. The propagation of errors in long term measurements of land atmosphere fluxes of carbon and water. *Global Change Biol.* 2, 231–240.
- Motulsky, H.J., Ransnas, L.A., 1987. Fitting curves to data using nonlinear regression: A practical and nonmathematical review. *FASEB J.* 1, 365–374.
- Nakane, K., 1994. Modelling the soil carbon cycle of pine ecosystems. *Ecol. Bull.* 43, 161–172.
- Norman, J.M., Garcia, R., Verma, S.B., 1992. Soil surface CO₂ fluxes and the carbon budget of grassland. *J. Geophys. Res.* 97, 18845–18853.
- Norman, J.M., Kucharik, C.J., Gower, S.T., Baldocchi, D.D., Crill, P.M., Rayment, M., Savage, K., Striegl, R.G., 1997. A comparison of six methods for measuring soil–surface carbon dioxide fluxes. *J. Geophys. Res.* 102, 28771–28777.
- Orchard, V.A., Cook, F.J., Corderoy, D.M., 1992. Field and laboratory studies on the relationships between respiration and moisture for two soils of contrasting fertility status. *Pedobiologia* 36, 21–33.
- Penning de Vries, F.W.T., 1975. The cost of maintenance processes in plant cells. *Ann. Bot.* 39, 77–92.
- Raich, J.W., Nadelhoffer, K.J., 1989. Belowground carbon allocation in forest systems: Global trends. *Ecology* 70, 1346–1354.
- Raich, J.W., Potter, C.S., 1995. Global patterns of carbon dioxide emissions from soils. *Global Biogeochem. Cycles* 9, 23–36.
- Raich, J.W., Schlesinger, W.H., 1992. The global carbon dioxide flux in soil respiration and its relationship to vegetation and climate. *Tellus* 44B, 81–99.
- Rayment, M.B., Jarvis, P.G., 1997. An improved open chamber system for measuring soil CO₂ effluxes in the field. *J. Geophys. Res.* 102, 28779–28784.
- Ryan, M.G., 1991. A simple method for estimating gross carbon budgets for vegetation in forest ecosystems. *Tree Physiol.* 9, 255–266.
- Schlesinger, W.H., 1997. *Biogeochemistry: An Analysis of Global Change*, Academic Press, San Diego, CA, 588pp.
- Schotanus, P., Nieuwstadt, F.T.M., de Bruin, H.A.R., 1983. Temperature measurement with a sonic anemometer and its application to heat and moisture fluxes. *Boundary Layer Meteorol.* 26, 81–93.
- Šimunek, J., Suarez, D.L., 1993. Modeling of carbon dioxide transport and production in soil. 1. Model development. *Water Resour. Res.* 29, 487–497.
- Singh, J.S., Gupta, S.R., 1977. Plant decomposition and soil respiration in terrestrial ecosystems. *Bot. Rev.* 43, 449–528.

- Smith, J.L., Paul, E.A., 1988. Use of an in situ labeling technique for the determination of seasonal ^{14}C distribution in Ponderosa pine. *Plant and Soil* 106, 221–229.
- Suarez, D.L., Šimunek, J., 1993. Modeling of carbon dioxide transport and production in soil. 2. Parameter selection, sensitivity analysis and comparison of model predictions to field data. *Water Resour. Res.* 29, 499–513.
- Timlin, D.J., Pachepsky, Y.A., 1996. Comparison of three methods to obtain the apparent dielectric constant from time domain reflectometry wave traces. *Soil. Sci. Soc. Am. J.* 60, 970–977.
- Vogt, K.A., Grier, C.C., Vogt, D.J., 1986. Production, turnover, and nutrient dynamics of above- and below-ground detritus of world forests. *Adv. Ecol. Res.* 15, 303–377.
- Waring, R.H., Law, B.E., Goulden, M.L., Bassow, S., McCreight, R.W., Wofsy, S.C., Bazzaz, F.A., 1995. Scaling gross ecosystem production at Harvard Forest with remote sensing: A comparison of estimates from a constrained quantum-use efficiency model and eddy correlation. *Plant, Cell, Environ.* 18, 1201–1213.
- Webb, E.K., Pearman, G.I., Leuning, R., 1980. Correction of flux measurements for density effects due to heat and water vapor transfer. *Quart. J.R. Meteorol. Soc.* 106, 85–100.
- Weber, M.G., 1985. Forest soil respiration in eastern Ontario Jack pine ecosystems. *Can. J. For. Res.* 15, 1069–1073.
- Wyngaard, J.C., 1974. On surface layer turbulence. In: Haugen, D. (Ed.), *Workshop on Micrometeorology*, Am. Meteorol. Soc., Boston, MA, pp. 101–149.